ORIGINAL ARTICLE

A C G publications

Org. Commun. 17:4 (2024) 218-240

organic communications

Synthesis, characterization, antioxidant, in silico-based virtual screening and anti-cancer potential of substituted 2-(4-acetyl-5-methyl-1h-1,2,3-triazol-1-yl)-n-phenylacetamide derivatives

Aiyagala M. M. Mallikarjunaswamy [1], Kuruvalli Gouthami [2], Subhasish Maity [2], Vaddi Damodara Reddy [2] and Lakshmi Basavegowda [1*]

[1] *Department of Chemistry, REVA University, Yelahanka, Bangalore 560064, India*
[2] *Department of Biotechnology, REVA University, Yelahanka, Bangalore 560064, India*

(Received December 06, 2024; Revised December 16, 2024; Accepted December 19, 2024)

Abstract: Cancer has been a widespread disease for decades in various of types for decades, and the search for effective treatments continues. Researchers are exploring various new drugs, including natural compounds and small organic molecules, for their potential to combat cancer. One promising approach involves hybrid structures that combine different pharmacophore units with known biological activities. These structures have gained popularity due to their encouraging results. In this study, we synthesized several new hybrid compounds containing 1,2,3-triazole units. We confirmed the structures of these compounds using methods like ^{1}H NMR, ^{13}C NMR, and LC-MS. We then evaluated their antioxidant properties and *in vitro* anticancer activities. The results showed that these new compounds demonstrated having good radical scavenging activity and potential agents for anticancer activity. Notably, compounds **3b**, **3d**, **3a**, **3m,** and **3i** exhibited low concentrations of IC_{50} values (14.08±0.6, 14.3±0.8, 15.82±0.4, 18.12±0.86 and 19.7±0.88 µg/mL, respectively) when compared to the standard drug Cisplatin (IC_{50}: 21.13±1.6 µg/mL). Computational analysis has been performed like ADMET evaluation and Molecular docking studies revealed the compounds having good binding affinity with cancer target proteins like HIF-1α ranging from -8.1 kcal/mol to -7.0 kcal/mol and HER2 ranging from -10.0 kcal/mol to -8.8 kcal/mol respectively when compared with standard drug Cisplatin showed binding affinity ranging from -4.2 kcal/mol to -3.9 kcal/mol.

Keywords: Nucleophilic substitution; 2-chloro-*N*-arylacetamide; 1,3-dipolar cycloaddition; 1,2,3-triazoles; ADMET properties; MTT Assay.

1. Introduction

Producing heterocyclic five-membered rings through 1,3-dipolar cycloaddition reactions with organoids is a significant focus in synthetic organic chemistry. 1,2,3- Triazoles are stable compounds interacting with biological targets by forming hydrogen bonds, making them important scaffolds in drug discovery.[1,2] Figure 1. Shows drugs containing the 1,2,3-triazole scaffold in their structure. 1,2,3-Triazoles derivatives are reported to have various pharmacological properties, including anticancer,[3-6] antimicrobial, [7] anti-inflammatory,[8,9] antitubercular, ten anti-HIV,[11] and antiviral effects.[12] Furthermore, compounds with the 1,2,3-triazoles group are used in industries as dyes, corrosion inhibitors, sensors, and photo stabilizers.[13] A remarkable fact is that 1,2,3-triazoles have a heat of formation of 272 KJ/mol, [14] and triazole-based salts find application as energetic materials.[15]

* Corresponding author:E-Mail: gouthamiv2023@yahoo.com

The article was published by ACG Publications
http://www.acgpubs.org/journal/organic-communications © October-December 2024 EISSN:1307-6175
DOI: http://doi.org/10.25135/acg.oc.177.2412.3374
Available online: December 30, 2024

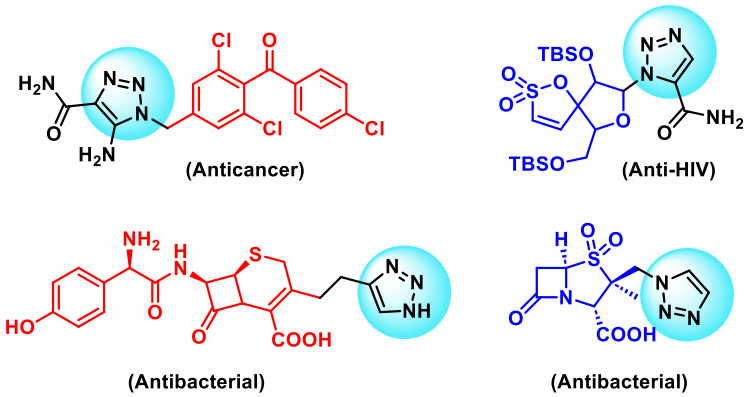

Figure 1. Biologically active 1,2,3-triazole drugs

The 1,2,3-triazole derivatives have been researched for a prolonged period, particularly in their application within oncological chemotherapy, as illustrated in Figure 2. Several organizations have examined deeply into this specialized domain. In one notable development, Rangappa et al. synthesized a series of 1,2,3-triazole-tethered 1,2-benzisoxazoles, revealing a remarkable cytostatic impact on human acute myeloid leukemia (AML) cells. Through the MTT assay, compound **1** emerged as the most potent antiproliferative agent against MV4-11 cells, boasting an IC_{50} of 2 μM.[16] Furthermore, the Miller group employed click chemistry to create a set of compounds designated as two and examined their antiproliferative efficacy.[17] Grymel et al. subsequently developed compound **3,** which exhibited an IC_{50} of 46 μM against MCF-7 breast cancer cells. In comparison, betulin demonstrated significant cytotoxicity, with antiproliferative effects of 30% on MCF-7 cells and 90% on HCT-116 cells after 48 hours of incubation.[18] Luan et al. also conducted additional research by synthesizing a 1,2,3-triazole compound, labeled as **4**, which showcased a broad-spectrum capacity to inhibit cell proliferation across six different cancer cell lines, with IC_{50} values ranging from 1.02 to 74.28 μM.[19] Gholampour et al. contributed to this body of work by creating novel 1,4-naphthoquinone-1,2,3-triazole hybrids. These compounds were tested for their anticancer properties on three human cancer cell lines: MCF-7, HT-29, and MOLT-4, with compound **5** standing out for its pronounced cytotoxicity. Notably, at concentrations of 10 and 20 μM, this compound induced cell cycle arrest in the G0/G1 phase.[20]

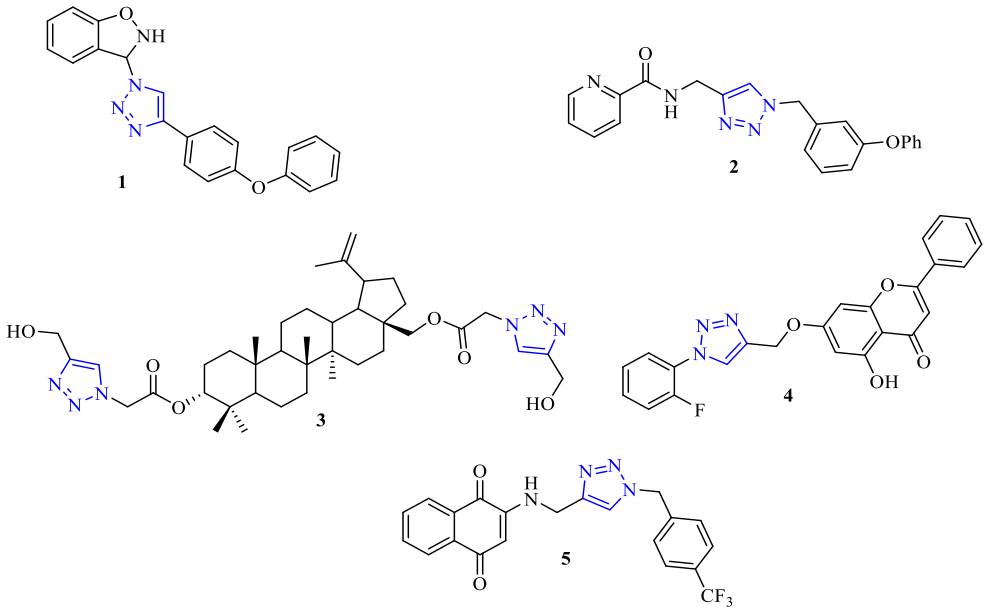

Figure 2. Representative derivatives of 1,2,3-triazoles with anti-anticancer activity

The 1,3-dipolar Huisgen cycloaddition reaction of azides and alkynes is the most common method for creating a 1,2,3-triazole framework.[21-23] However, the initial Huisgen cycloaddition reaction

required a strong electron-withdrawing substituent on either the azide or the alkyne. These reactions were frequently carried out at high temperatures for extended periods, resulting in the separation of mixtures of 1,4- and 1,5-disubstituted regioisomers,[24] and the electronic effects of the substituent groups on the phenyl ring were not well known. Friedel-Crafts acylation is another key process for producing aryl ketones.[25]

Triazoles can also synthesized by cycloaddition of azides with electron-deficient alkenes, metal acetylides, alkynic Grignard reagents, phosphonium salts, and other substituted alkynes.[26-30] Organic azides (such as trimethylsilyl, alkyl, allyl, and aryl azides), metal azides, or hydrazoic acid are frequently utilized in cycloaddition reactions involving alkynes.[31-34] Triazoles can be produced on solid substrates such as polymer or resin-bound azides, alkynes, enamines, or β-ketoamides. [35-38] Wang et al. and Ju and co-workers have also demonstrated 1,3-dipolar cycloaddition processes in water that do not require a catalyst.[39-40] Sharpless and co-worker's[41-42] innovated the synthesis of triazoles by employing in situ generated Cu(I) derived from copper sulfate and sodium ascorbate, a stoichiometric amount of copper turnings in aqueous conditions, all maintained at ambient temperature. The utilization of copper nanoclusters [43] and Cu(I) salts[44-45] in conjunction with nitrogenous bases was also reported for the synthesis of 1,2,3-triazoles, although the latter approach yielded side products such as diacetylenes and bis-triazoles. Orgueira et al.[46] reported the cycloaddition of terminal alkynes and azides using in situ generated Cu(I) from Cu (0) nanoscale-activated powder in the presence of amine hydrochloride salt. More recently, three-component coupling reactions have been utilized for triazole synthesis, leveraging catalysts such as monometallic palladium,[47] bimetallic Pd(0)–Cu(I),[48] microwave-assisted Cu(0)–Cu(II),[49] and Cu(II)–sodium ascorbate-L-proline.[50] Notably, the microwave-assisted synthesis method significantly reduced reaction times from 12–48 hours to 10–15 minutes, although with an elevated temperature of 125°C during microwave irradiation.

As part of our continued interest in expanding the structural diversity of the 1,2,3-triazole products herein, we report our new results regarding the synthesis of 2-(4-acetyl-5-methyl-1H-1,2,3-triazol-1-yl)-N-phenylacetamide via one-pot three-component reaction of 2-chloro-N-phenylacetamide, sodium azide and active methylene ketones in the presence of base under the reflux condition.

2. Experimental

2.1. Materials and Methods

All the chemicals were obtained from commercial suppliers and used without further purification. The reactions were conducted in oven-dried glass wares and maintained under the appropriate atmospheric conditions. To monitor the progress of the reactions, thin-layer chromatography (TLC) was employed, specifically, 0.25 mm Merck Silica gel 60 F254 plates were used, and visualization was achieved using UV light. Column chromatography used 60-120 mesh silica gel as the stationary phase. Elution was carried out using a mixture of hexane and ethyl acetate as the mobile phase. NMR spectra were recorded on a Jeol ECZ 400R spectrometer (^{1}H at 400 MHz and ^{13}C at 100 MHz) using DMSO-d_6 as the solvent with TMS as the internal standard. Chemical shifts (δ) are reported relative to residual solvent signals (DMSO-d_6, 2.5 ppm for ^{1}H NMR and triplet centered at 39.5 ppm for ^{13}C NMR). Liquid chromatography mass spectrometric analysis was carried out in ESI quadrupole time of flight Agilent mass spectrometer.

2.2. Chemistry

*2.2.1. General procedure for the preparation of 2-(4-acetyl-5-methyl-1H-1,2,3-triazole-1-yl)-N-phenylacetamide (**3a- 3p**)*

To a solution of 2-chloro-N-arylacetamide **1a** (1.0 mmol) in ethanol: water (1:1), NaN_3 (0.10g, 1.5 mmol), acetylacetone (0.08g, 1.1 mmol) and K_2CO_3 (0.15g, 1.1 mmol) was added the resulting mixture was stirred in an oil bath at 80^{o}C for 2 hours. After completion of the reaction, as monitored by thin-layer chromatography, the reaction mixture was cooled to RT and poured into ice-cold water. The product that precipitated out was filtered, washed successively with ice-cold water, and purified by

column chromatography on silica gel (60-120 mesh) with ethyl acetate-petroleum ether mixture (40:60) as the eluting solvent to obtain the desired product.

*2-(4-acetyl-5-methyl-1H-1,2,3-triazol-1-yl)-N-phenylacetamide (**3a**)*: White solid; Yield: 98%; ^{1}H NMR (400 MHz, DMSO-d_6): δ 10.54 (s, 1H, NH), 7.57 (d, *J* = 7.7 Hz, 2H, Ar), 7.33 (t, *J* = 7.9 Hz, 2H, Ar), 7.09 (t, *J* = 7.4 Hz, 1H, Ar), 5.37 (s, 2H, CH_2), 2.58 (s, 3H, CH_3), 2.50 (s, 3H, CH_3); ^{13}C NMR (100 MHz, DMSO-d_6): δ 193.8, 164.1, 143.1, 139.0, 138.7, 129.4, 124.4, 119.8, 50.7, 27.9, 9.3; LCMS (ESI): $C_{13}H_{14}N_4O_2$ [M-H]$^+$; calculated: 257.28; found: 257.00.

*2-(4-acetyl-5-methyl-1H-1,2,3-triazol-1-yl)-N-(4-fluorophenyl)acetamide (**3b**)*: White solid; Yield: 96%; ^{1}H NMR (400 MHz, DMSO-d_6): δ 7.60 (d, *J* = 8.7 Hz, 2H, Ar), 7.39 (d, *J* = 8.7 Hz, 2H, Ar), 5.38 (s, 2H, CH_2), 2.58 (s, 3H, CH_3), 2.50 (s, 3H, CH_3); ^{13}C NMR (100 MHz, DMSO-d_6): δ 193.8, 164.3, 143.1, 139.1, 137.7, 129.3, 128.0, 121.4, 50.6, 27.9, 9.2; LCMS (ESI): $C_{13}H_{13}FN_4O_2$ [M+H]$^+$; calculated: 277.27; found: 277.00.

*2-(4-acetyl-5-methyl-1H-1,2,3-triazol-1-yl)-N-(3-chlorophenyl)acetamide (**3c**):* White solid; Yield: 97%; ^{1}H NMR (400 MHz, DMSO-d_6): δ 10.53 (s, 1H, NH), 7.44 – 7.34 (m, 2H, Ar), 7.22 (t, *J* = 7.8 Hz, 1H, Ar), 6.92 (d, *J* = 7.4 Hz, 1H, Ar), 5.38 (s, 2H, CH_2), 2.59 (s, 3H, CH_3), 2.28 (s, 3H, CH_3); ^{13}C NMR (100 MHz, DMSO-d_6): δ 193.8, 164.0, 160.0, 157.6, 143.1, 139.0, 135.1, 121.7, 121.6, 115.9, 50.6, 27.9, 9.2; LCMS (ESI): $C_{13}H_{13}ClN_4O_2$ [M+H]$^+$; calculated: 293.07; found: 293.00.

*2-(4-acetyl-5-methyl-1H-1,2,3-triazol-1-yl)-N-(2,6-dimethylphenyl)acetamide (**3d**)*: White solid; Yield: 95%; ^{1}H NMR (400 MHz, DMSO-d_6): δ 9.84 (s, 1H, NH), 7.06 (s, 3H, Ar), 5.42 (s, 2H, CH_2), 2.56 (s, 3H, CH_3), 2.50 (s, 3H, CH_3), 2.15 (s, 6H, CH_3).; ^{13}C NMR (100 MHz, DMSO-d_6): δ 193.8, 164.0, 143.2, 138.8, 135.5, 134.6, 128.3, 127.3, 50.0, 27.0, 18.5, 9.2; LCMS (ESI): $C_{15}H_{18}N_4O_2$ [M+H]$^+$; calculated: 287.33; found: 287.00.

*2-(4-acetyl-5-methyl-1H-1,2,3-triazol-1-yl)-N-(2-fluorophenyl)acetamide (**3e**)*: White solid; Yield: 97%; ^{1}H NMR (400 MHz, DMSO-d_6): δ 7.87 (t, *J* = 7.5 Hz, 1H, Ar), 7.28 (dd, *J* = 12.2, 6.5 Hz, 1H, Ar), 7.13 – 7.22 (m, 2H, Ar), 5.46 (s, 2H, CH_2), 2.58 (s, 3H, CH_3), 2.50 (s, 3H, CH_3); ^{13}C NMR (100 MHz, DMSO-d_6): δ 193.8, 164.7, 143.2, 139.0, 126.2, 126.0, 124.9, 124.4, 116.2, 116.0, 50.5, 27.9, 9.2; LCMS (ESI): $C_{13}H_{13}FN_4O_2$ [M+H]$^+$; calculated: 277.10; found: 277.00.

*2-(4-acetyl-5-methyl-1H-1,2,3-triazol-1-yl)-N-(4-chlorophenyl)acetamide (**3f**):* White solid; Yield: 95%; ^{1}H NMR (400 MHz, DMSO-d_6): δ 7.60 (d, *J* = 8.7 Hz, 2H, Ar), 7.39 (d, *J* = 8.7 Hz, 2H, Ar), 5.38 (s, 2H, CH_2), 2.58 (s, 3H, CH_3), 2.50 (s, 3H, CH_3); ^{13}C NMR (100 MHz, DMSO-d_6): δ 193.8, 164.3, 143.1, 139.1, 137.7, 129.3, 128.3, 121.4, 50.6, 27.9, 9.2; LCMS (ESI): $C_{13}H_{13}ClN_4O_2$ [M+H]$^+$; calculated: 293.72; found: 293.00.

*2-(4-acetyl-5-methyl-1H-1,2,3-triazol-1-yl)-N-(2-chlorophenyl)acetamide (**3g**)*: White solid; Yield: 96%; ^{1}H NMR (400 MHz, DMSO-d_6): δ 10.19 (s, 1H, NH), 7.70 (d, *J* = 7.8 Hz, 1H, Ar), 7.53 (d, *J* = 7.8 Hz, 1H, Ar), 7.21 – 7.35 (m, 2H, Ar), 5.48 (s, 2H, CH_2), 2.58 (s, 3H, CH_3), 2.50 (s, 3H_3); ^{13}C NMR (100 MHz, DMSO-d_6): δ 193.8, 164.8, 143.2, 139.0, 134.5, 130.0, 128.1, 127.4, 127.1, 126.6, 50.4, 27.9, 9.2; LCMS (ESI): $C_{11}H_9ClN_6O$ [M+H]$^+$; calculated: 293.72; found: 293.00.

*2-(4-acetyl-5-methyl-1H-1,2,3-triazol-1-yl)-N-(4-methoxyphenyl)acetamide (**3h**)*: White solid; Yield: 95%; ^{1}H NMR (400 MHz, DMSO-d_6): δ 10.44 (s, 1H, NH), 7.49 (d, *J* = 7.3 Hz, 2H, Ar), 6.90 (d, *J* = 7.3 Hz, 2H, Ar), 5.34 (s, 2H, CH_2), 3.71 (s, 3H, OCH_3), 2.58 (s, 3H, CH_3), 2.50 (s, 3H, CH_3); ^{13}C NMR (100 MHz, DMSO-d_6): δ 193.8, 163.6, 156.1, 143.1, 139.0, 131.8, 121.3, 114.5, 55.6, 50.6, 27.9, 9.2; LCMS (ESI): $C_{14}H_{16}N_4O_3$ [M-H]$^+$; calculated: 287.30; found: 287.00.

*2-(4-acetyl-5-methyl-1H-1,2,3-triazol-1-yl)-N-(3,5-chlorophenyl)acetamide (**3i**)*: White solid; Yield: 92%; ^{1}H NMR (400 MHz, DMSO-d_6): δ 10.95 (s, 1H, NH), 7.63 (s, 2H, Ar), 7.34 (s, 1H, Ar), 5.42 (s, 2H, CH_2), 2.60 (s, 3H, CH_3), 2.51 (s, 3H, CH_3); ^{13}C NMR (100 MHz, DMSO-d_6): δ 193.7, 164.9, 143.1,

141.0, 139.1, 134.7, 123.7, 118.0, 50.7, 27.9, 9.2; LCMS (ESI): $C_{13}H_{12}Cl_2N_4O_2$ $[M-H]^+$; calculated: 325.03; found: 325.00.

*2-(4-acetyl-5-methyl-1H-1,2,3-triazol-1-yl)-N-(p-tolyl)acetamide (**3j**)*: White solid; Yield: 95%; ^{1}H NMR (400 MHz, DMSO-d_6): δ 10.48 (s, 1H, NH), 7.46 (d, J = 8.3 Hz, 2H, Ar), 7.14 (d, J = 8.2 Hz, 2H, Ar), 5.35 (s, 2H, CH_2), 2.58 (s, 3H, CH_3), 2.50 (s, 3H, CH_3), 2.26 (s, 3H, CH_3); ^{13}C NMR (100 MHz, DMSO-d_6): δ 193.8, 163.8, 143.1, 139.0, 136.2, 133.4, 129.8, 119.8, 50.6, 27.9, 20.9, 9.3; LCMS (ESI): $C_{14}H_{16}N_4O_2$ $[M+H]^+$; calculated: 273.30; found: 273.00.

*2-(4-acetyl-5-methyl-1H-1,2,3-triazol-1-yl)-N-(4-bromophenyl)acetamide (**3k**)*: White solid; Yield: 93%; ^{1}H NMR (400 MHz, DMSO-d_6): δ 10.77 (s, 1H, NH), 7.53 (t, J = 6.9 Hz, 4H, Ar), 5.39 (s, 2H, CH_2), 2.59 (s, 3H, CH_3), 2.50 (s, 3H, CH_3).; ^{13}C NMR (100 MHz, DMSO-d_6): δ 193.8, 164.3, 139.1, 137.7, 129.3, 128.8, 121.4, 50.6, 27.9, 9.2; LCMS (ESI): $C_{13}H_{13}BrN_4O_2$ $[M+H]^+$; calculated: 339.17; found: 339.00.

*2-(4-acetyl-5-methyl-1H-1,2,3-triazol-1-yl)-N-(m-tolyl)acetamide (**3l**)*: White solid; Yield: 96%; ^{1}H NMR (400 MHz, DMSO-d_6): δ 10.53 (s, 1H, NH), 7.43 (s, 1H, Ar), 7.36 (d, J = 8.1 Hz, 1H, Ar), 7.22 (t, J = 7.8 Hz, 1H, Ar), 6.92 (d, J = 7.4 Hz, 1H, Ar), 5.38 (s, 2H, CH_2), 2.59 (s, 3H, CH_3), 2.51 (s, 3H, CH_3), 2.28 (s, 3H, CH_3); ^{13}C NMR (100 MHz, DMSO-d_6): δ 193.8, 164.0, 143.1, 139.0, 138.6, 129.2, 125.1, 120.3, 117.0, 50.7, 27.9, 21.6, 9.2; LCMS (ESI): $C_{14}H_{16}N_4O_2$ $[M+H]^+$; calculated: 273.30; found: 273.00.

*2-(4-acetyl-5-methyl-1H-1,2,3-triazol-1-yl)-N-(2,4-dimethylphenyl)acetamide (**3m**)*: White solid; Yield: 94%; ^{1}H NMR (400 MHz, DMSO-d_6): δ 7.57 (d, J = 8.0 Hz, 1H, Ar), 7.37 – 7.25 (m, 2H, Ar), 5.71 (s, 2H, CH_2), 2.89 (s, 3H, CH_3), 2.82 (s, 3H, CH_3), 2.55 (s, 3H, CH_3), 2.50 (s, 3H, CH_3); ^{13}C NMR (100 MHz, DMSO-d_6): δ 193.8, 164.3, 143.2, 138.9, 135.3, 133.3, 132.2, 131.4, 127.0, 120.4, 50.4, 27.9, 20.9, 18.2, 9.2; LCMS (ESI): $C_{15}H_{18}N_4O_2$ $[M+H]^+$; calculated: 287.33; found: 287.00.

*2-(4-acetyl-5-methyl-1H-1,2,3-triazol-1-yl)-N-(o-tolyl)acetamide (**3n**)*: White solid; Yield: 96%; ^{1}H NMR (400 MHz, DMSO-d_6): δ 10.52 (s, 1H, NH), 7.33 – 7.44 (m, 2H, Ar), 7.21 (t, J = 7.8 Hz, 1H, Ar), 6.91 (d, J = 7.4 Hz, 1H, Ar), 5.37 (s, 2H, CH_2), 2.58 (s, 3H, CH_3), 2.50 (s, 3H, CH_3), 2.27 (s, 3H, CH_3).; ^{13}C NMR (100 MHz, DMSO-d_6): δ 193.8, 164.0, 143.1, 139.0, 138.6, 129.2, 125.1, 120.3, 117.0, 50.7, 27.9, 21.6, 9.2; LCMS (ESI): $C_{14}H_{16}N_4O_2$ $[M+H]^+$; calculated: 273.3021; found: 273.00.

2.3. Biology

2.3.1. Antioxidant Capacity Assays

2.3.1.1. DPPH Radical Scavenging Activity

The compounds synthesized with 1,2,3 triazoles were evaluated by $DPPH^+$ radical scavenging activity. Ascorbic acid was dissolved in methanol to serve as a positive control, and sample solutions were prepared at concentrations of 5, 10, 20, 50, and 100 µg/mL. Following the transfer of the sample solution into a clean tube, one milliliter of 0.25% $DPPH^+$ was added at varying concentrations. The mixture was then incubated at 37°C for 30 minutes. The absorbance of the reaction solution was measured using a UV-Vis spectrophotometer at a wavelength of 515 nm.[51] The experiment was conducted in triplicate. The scavenging activity of free radicals was calculated using the following formula:

$$\% \text{ Scavenging} = [(A_0 - A_1) / A_0] \times 100$$

Where A_0 is the absorbance of the control, and A_1 is the absorbance of extract/standard taken as Ascorbic acid.

2.3.1.2. ABTS Assay

The $ABTS^+$ assay depends on the absorption of light by $ABTS^+$ radicals, and it was carried out using well-established methods described in earlier writings.[52] An antioxidant that can provide a hydrogen atom will inactivate a stable free radical, causing a shift in absorption that can be tracked using spectroscopy. The relatively stable $ABTS^+$ radical has a green color and can be quantified using spectrophotometry at 734 nm. Following the combination of an equal quantity of $ABTS^+$ with APS and allowing the mixture to rest in darkness at room temperature for 14-16 hours, $ABTS^+$ radical cations were generated. Subsequently, the solution was diluted further with methanol (in a 1:60 ratio) until an absorbance of 1.00 at 734 nm was attained using a spectrophotometer. The $ABTS^+$ working solution was mixed with varying concentrations of the test sample and the reference standard, up to 50 ml, to reach a final volume of 1ml, totaling 950 mL. The absorbance at 734nm was promptly measured. Graph Pad Prism software was utilized for the analysis to ascertain the percent inhibition and IC_{50} values at different doses. The supplied formula was used to compute the percentage inhibition of growth:

$$\% \text{ Inhibition} = \frac{(\text{Absorbance of Control} - \text{Absorbance of Sample})}{(\text{OD of Control}) \times 100}$$

2.3.1.3. MTT Assay

Cells were inoculated into a 96-well flat-bottom microtiter plate at a density of 1 x 10^4 cells per well and permitted to adhere for a 24 hours at 37°C within a CO_2 incubator. Following this 24-hour incubation period, the culture medium was substituted with fresh medium. The cells were subsequently exposed to different concentrations ranging from 2.5 to 50µg/mL of the synthesized compound for a duration of 24 hours at a temperature of 37°C within a CO_2 incubator. Following a 24-hour incubation period, the culture medium was substituted with a new medium. Thereafter, 10 µL of the MTT working solution (5mg/ml) in phosphate buffer solution) was introduced into each well, and the plate was incubated for 4 hours at 37°C within a CO_2 incubator. The medium was subsequently aspirated, and the resulting formazan crystals were dissolved by adding 50 µL of DMSO to each well, followed by incubation for 30 minutes at 37°C in a CO_2 incubator. The concentration of the dissolved formazan crystals, characterized by their purple hue, was measured using the ELISA plate reader at a wavelength of 540 nm.[53-54]

2.3.2. In-silico Studies

2.3.2.1. Selection of 1,2,3 Triazoles Synthesized Compounds for Inhibitory Design

1,2,3 Triazoles synthesized compound structures were found and then converted to mol files by using Chem sketch and to protein databank (PDB) format using PyMOL for further analysis. The reference chemical structure of Cisplatin downloaded the structure data format (SDF) file from the PubChem-NCBI database.[55]

2.3.2.2. Drug Likeliness Prediction of 1,2,3 Triazoles Synthesized Compounds

Using Molinspiration, drug-likeliness properties of the phytochemicals are done (Molinspiration Cheminformatics). The Lipinski rule provides the drug-likeness properties such as less than 500 g/mol of molecular weight, less than 10 H-bond acceptors, and less than 5 H-bond donors. The presence of H-bond donors and acceptors in a therapeutic agent's structure is essential for drug-protein interactions, distribution, membrane transport, and aqueous solubility.[56]

2.3.2.3. ADMET Properties

By using admetSAR online server the ADME and toxicity of the 1,2,3 Triazoles synthesized compounds are predicted (http://lmmd.ecust.edu.cn/admetsar2/). The ADMET properties are

considering the parameters of Androgen receptor binding, Aromatase binding, CYP3A4 substrate, Estrogen receptor binding, Glucocorticoid receptor binding, Human Intestinal Absorption, OATP1B1 inhibitor, reproductive toxicity, Respiratory toxicity and UGT catalysed is considered the best active molecules and screen experimentally using molecular docking.[57]

2.3.2.4. Identification of Protein Targets and Homology Model Construction

The proteins such as HIF-1α and HER2 were recovered by running protein BLAST submitted in NCBI. These protein query sequences were submitted to CastP server, to search for evolutionary-related protein structures using BLAST and HHblits method. This provides the description of length, sequence ID, percentage of identity, sequence coverage and total score. CastP calculation server were used for the prediction of active site amino acids (http://sts.bioe.uic.edu/castp/calculation.html) according to the 3D protein structure's defining measures of surface area and surface volume.[58]

2.3.2.5. Macromolecule Preparation

The macromolecules selected for docking studies are HIF-1α (PDB Id:1H2N, resolution factor: 2.84 Å) and HER2 (PDB Id:3PP0, resolution factor: 2.25 Å) are obtained from the protein data bank (PDB). Making use of the Biovia Discovery Studio visualizer tool, the macro molecules have been converted into pdb format, and docking studies were conducted utilizing 3D structure Figure 3 (a-b). A program called Auto Dock Vina 4.2 is used in molecular docking studies to forecast the interactions between protein targets and ligands. A protein-ligand interaction's binding affinity and bond length will be examined. The function of the transcription factor hypoxia-inducible factor (HIF) is modulated by hydroxylation that is dependent on oxygen levels. This regulation influences how tumor cells react to variations in oxygen concentration. HIF-1α is crucial in the context of cancer biology.[59] Abnormal signaling of members of the ErbB family, specifically HER2, is associated with various human cancers. Furthermore, the expression of HER2 serves as a predictor for disease recurrence and prognosis in patients.[60]

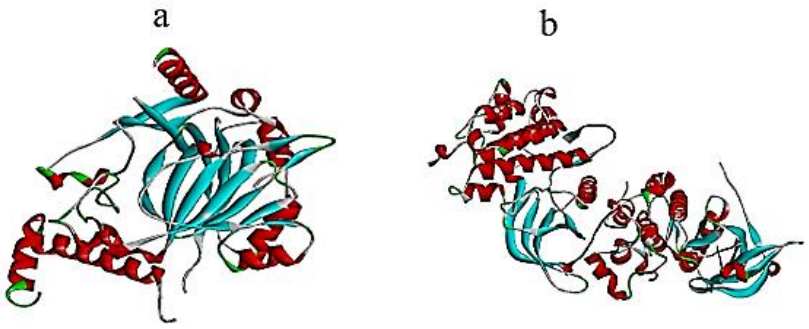

HIF-1α (PDB Id:1H2N) HER2 (PDB Id:3PP0)

Figure 3 (a-b). Representation of 3D model of selected proteins.

3. Results and Discussion

3.1. Chemistry

The chemical synthesis of 2-(4-acetyl-5-methyl-1H-1,2,3-triazol-1-yl)-N-phenylacetamide (**3a**) was initiated by a retrosynthetic analysis, as given in (Scheme 1). 2-azido-N-phenylacetamide (**2a**) is one of the important intermediates in the synthesis of compound (**3a)**, which was readily derived from 2-chloro-N-phenylacetamide form (**1a**). The intermediate (**2a)** was prepared by reacting 2-chloroacetyl chloride with aniline followed by nucleophilic substitution with sodium azide. Using 2-azido-N-phenylacetamide as a key intermediate, the synthesis proceeded towards the desired product, 2-(4-acetyl-5-methyl-1H-1,2,3-triazol-1-yl)-N-phenylacetamide (**3a**). To construct the 1,2,3-triazole core,

was performed between 2-azido-N-phenylacetamide and acetyl acetone. The active methylene ketone undergoes keto enol tautomerism to form to form intermediate enolate, generated in situ, and 2-azido-N-phenylacetamide underwent a 1,3-dipolar cycloaddition to produce the target molecule.

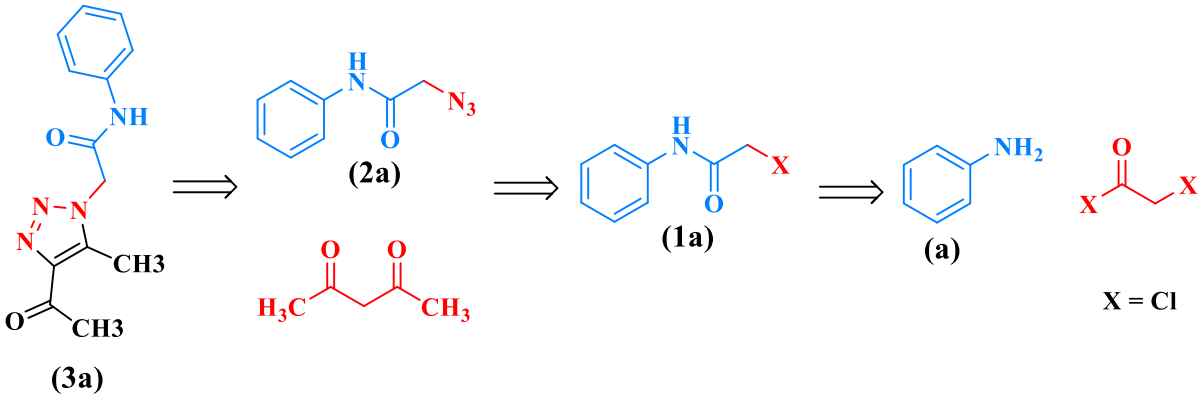

Scheme 1. Retrosynthetic route for acetamide derivatives of 1,2,3-triazoles

A series of new simple, rapid, eco-friendly one-pot multicomponent synthesis of substituted 2-(4-acetyl-5-methyl-1H-1,2,3-triazol-1-yl)-N-phenylacetamide (**3a**) from 2-chloro-N-phenylacetamide(**1a**), sodium azide and active methylene ketone in the presence of potassium carbonate under heating condition in ethanol/water was executed (Scheme 2). The reaction proceeds via 1,3-dipolar-cycloaddition. Our maiden studies commenced with the reaction of 2-chloro-N-phenylacetamide (**1a**) and sodium azide in different solvent conditions at 80°C, which yielded 2-azido-N-phenylacetamide (**2a**) as an intermediate in 3 hours (Table 1). Further, active methylene ketone was added to the same reaction mixture and refluxed for 12 hours, but no progress was observed to formation of desired product (**3a**). However, when a base was added, the reaction reached completion within 45 minutes. This finding encouraged us to conduct the reaction under basic conditions.

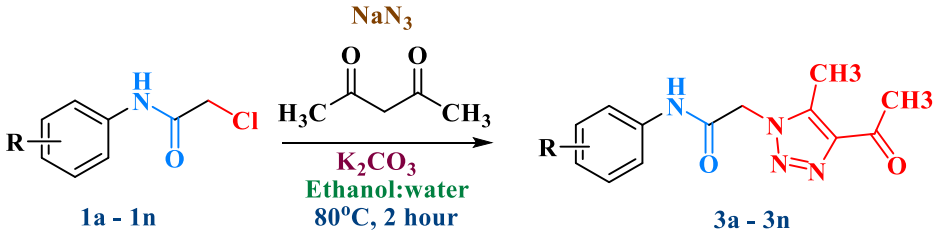

Scheme 2. 2-(4-acetyl-5-methyl-1H-1,2,3-triazol-1-yl)-N-phenylacetamide via a one-pot, three-component reaction of 2-chloro-N-phenylacetamide, sodium azide and active methylene ketones

Based on this observation, we optimized the one-pot reaction conditions using various bases and solvents to explore the substrate scope. The results are summarized in (Table 1). The role of the base was investigated about the formation of product **3a** from the corresponding haloacetamide (**1a**), where active methylene ketone was generated by the base to promote the cyclization of 2-azido-N-phenylacetamide (**2a**). Various bases were tested using the model substrate 2-chloro-N-phenylacetamide (Table 1, Entries 1-10).

The reaction performed poorly with organic weak and moderate bases in both protic and aprotic solvents over 4-6 hours (Table 1, Entries 11-18). Using the nucleophilic base NaH also yielded unsatisfactory results in THF, and moderate results with NaOMe and K^{t}OBu in suitable protic solvents (Table 1, Entries 5-7). However, the reaction courses improved significantly with non-nucleophilic bases, yielding satisfactory results. Specifically, Na_2CO_3 and $NaHCO_3$ provided yields of up to 80% and 76% of the desired product, respectively (Table 1, Entries 9 and 10). The milder non-nucleophilic base

K_2CO_3 in ethanol gave an impressive overall yield of 94% in just 2 hours (Table 1, Entry 8). Therefore, the inexpensive K_2CO_3, which afforded excellent results, was selected for reactions with other 2-chloro-N-phenylacetamides.

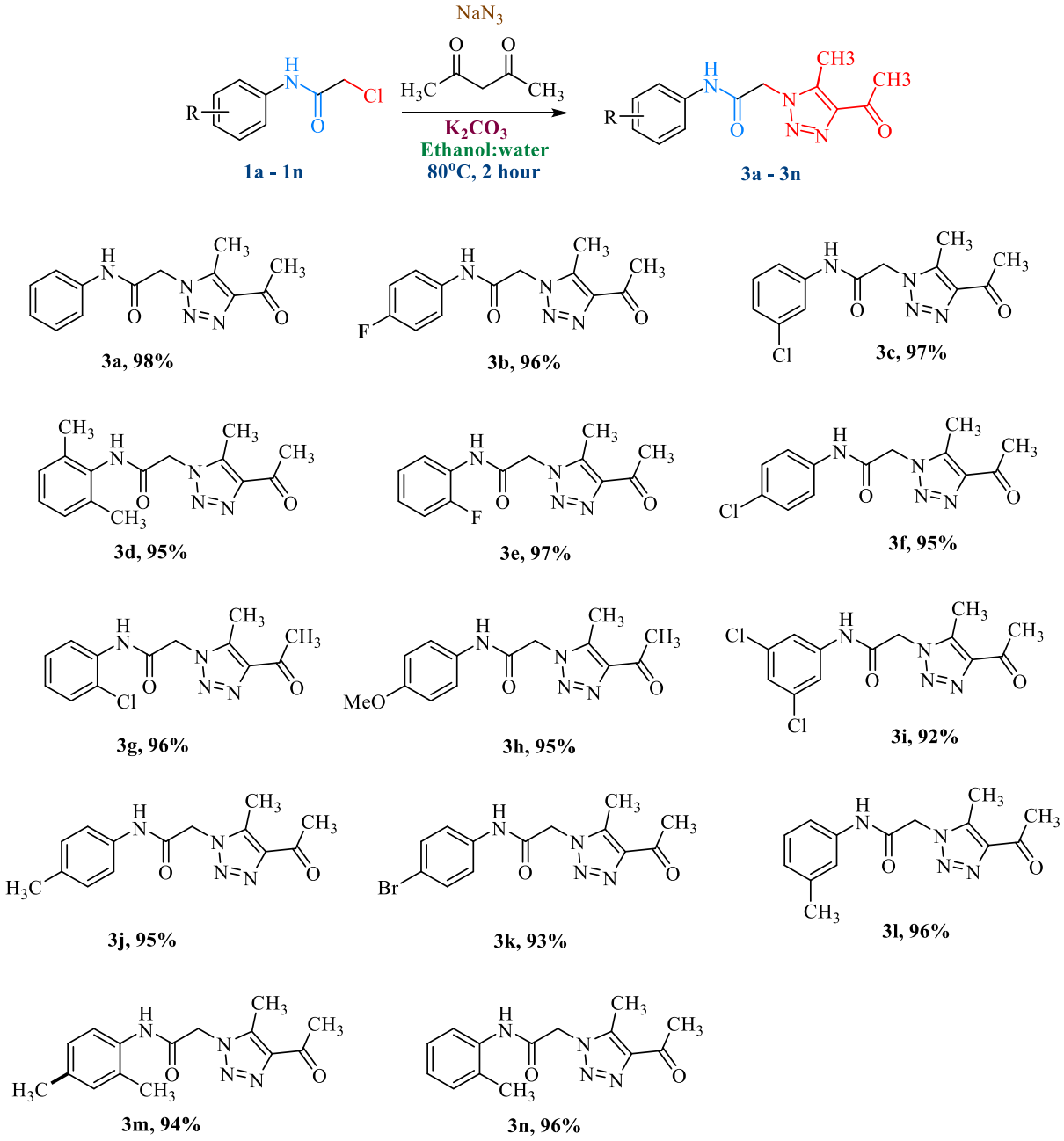

Figure 4. Synthesized substituted 2-(4-acetyl-5-methyl-1H-1,2,3-triazol-1-yl)-N-phenylacetamide

Assuming the existence of the charged species 2-azido-N-phenylacetamide and active methylene ketone as dipolar intermediates through which the reaction proceeds, polar solvents are expected to facilitate the reaction due to their hydrogen interactions. Therefore, we screened solvents for the transformation of 2-chloro-N-phenylacetamide to 2-(4-acetyl-5-methyl-1H-1,2,3-triazol-1-yl)-N-phenylacetamide (Table 1, Entries 1-19). When the reaction was performed in the non-polar solvent toluene at 100°C and ether solvents such as THF or 1,4-dioxane at 60°C for 8 hours, the yields were not satisfactory (Table 1, Entries 11 & 12). However, using the polar aprotic solvents DMF or DMSO, there was a significant increase in the reaction rate and yields. The dielectric polar aprotic solvent acetonitrile

also gave satisfactory yields (Table 1, Entries 13-15), providing an opportunity to improve the reactions further. The results were highly impressive with the greener solvent water, although the reaction took longer to complete. An attempt with an ethanol: water (1:2) mixture gave excellent results at both 80°C and 100°C in a shorter reaction time.

Temperature is found to be a significant factor in the reaction. No progress was observed when the reaction was performed at room temperature, and it could not proceed to any extent even after 12 hours at this temperature. High conversions were witnessed at 50°C, with reaction times reducing from 10 hours at 50°C to just 2 hours at 80°C or 100°C. Reactions at higher temperatures provided a significantly larger concentration of reactant molecules capable of crossing the energy barrier to form the desired product. Excellent yields were achieved in all cases with short reaction times. Aromatic amides containing both electron-withdrawing and electron-donating groups provided yields of up to 97%. The scalability of the reaction was examined by converting one gram of 2-chloro-N-phenylacetamide to 2-(4-acetyl-5-methyl-1H-1,2,3-triazol-1-yl)-N-phenylacetamide, yielding 98% (Figure 4).

Table 1. Optimization of one-pot synthesis of 2-(4-acetyl-5-methyl-1H-1,2,3-triazol-1-yl)-N-phenylacetamide from 2-chloro-N-phenylacetamide*

Entry	Base	Solvent	Temp(ºC)	Time(Hr)	Yield(%)
1	TEA	EtOH/DCM	80/40	6	45
2	DIPEA	EtOH	80	5	45
3	DMAP	EtOH	80	4	48
4	Pyridine	DCM	40	4	53
5	NaH	THF	0-RT	5	35
6	NaOMe	MeOH	60	3	70
7	K^{t}OBu	^{t}BuOH	80	3	66
8	K_2CO_3	EtOH	80	2	94
9	Na_2CO_3	EtOH	80	2	80
10	$NaHCO_3$	EtOH	80	2	75
11	K_2CO_3	Toluene	100	8	35
12	K_2CO_3	1,4 Dioxane/THF	60	8	40
13	K_2CO_3	Acetonitrile	80	4	82
14	K_2CO_3	DMSO	100	3	80
15	K_2CO_3	DMF	100	3	82
16	K_2CO_3	Water	100	8	90
17	K_2CO_3	EtOH: Water	80	2	98
18	K_2CO_3	EtOH: Water	RT	12	NR
19	K_2CO_3	EtOH: Water	50	10	88

*2-Chloro-N-phenylacetamide (1.0 mmol), Sodium azide (1.5 mmol), acetyl acetone (1.1 mmol), Base (1.1mmol), Solvent (10 mL)

The proposed reaction mechanism of this three-component reaction (Scheme 3) involves active methylene ketone undergo keto-enol tautomerism to form the intermediate enolate **II** in the presence of K_2CO_3. Cyclization of 2-azido-N-phenylacetamide **I** with enolate **II** affords the intermediate **III**. Finally, dehydration of **III** results in the formation of the desired 1,2,3-triazoles (Scheme 3).

Synthesis,substituted 2-(4-acetyl-5-methyl-1h-1,2,3-triazol-1-yl)-n-phenylacetamides

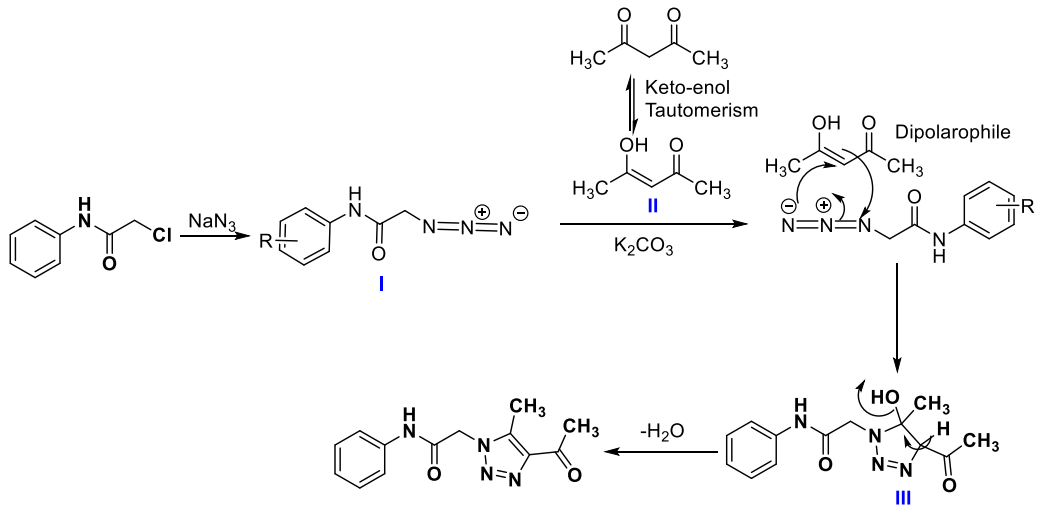

Scheme 3. Proposed reaction mechanism for 2-(4-acetyl-5-methyl-1H-1,2,3-triazol-1-yl)-N-phenylacetamide

3.2. Biology

3.2.1. In vitro Studies

3.2.1.1. Antioxidant Activity Assays

The activities of radical scavenging hold considerable importance owing to the harmful effects of free radicals within biological systems.[61] The *in vitro* antioxidant capabilities of the newly synthesized compounds containing 1,2,3-triazoles were assessed at various concentrations (5, 10, 20, 50, and 100 µg/mL) using established assays such as the $DPPH^+$ and $ABTS^+$ free radical scavenging methods. The $ABTS^+$ assay is characterized by the production of a blue/green $ABTS^+$ compound, which can be reduced by antioxidants. In contrast, the $DPPH^+$ assay relies on the conversion of the purple $DPPH^+$ to 1,1-diphenyl-2-picryl hydrazine. The influence of antioxidants on $DPPH^+$ radicals is attributed to their capacity to donate hydrogen.

Table 2. IC_{50} values for $DPPH^+$ and $ABTS^+$ results

	$DPPH^+$	**$ABTS^+$**
Compounds	**IC_{50} (µg/mL)**	**IC_{50} (µg/mL)**
3a	27.2 ±2.3	30.2±2.0
3b	28.00±0.8	33.28±2.34
3c	21.69±0.66	32.82±0.58
3d	31.81±1.9	24.95±0.8
3e	32.29±2.9	19.1±2.1
3f	30.8±0.88	23.8±1.89
3g	31.30±1.4	23.88±0.64
3h	28.8±1.8	24.9±2.14
3i	27.56±0.78	35.82±2.6
3j	30.76±0.5	32.3±1.56
3k	31.41±1.6	25.86±0.88
3l	28.7±2.1	15.6±1.8
3m	29.6±0.56	22.5±2.4
3n	32.43±1.89	22±0.8
Ascorbic acid	16.94±2.2	-
Gallic acid	-	6.2±0.67

Values are mean ± SD of three independent experiments

The evaluation of anti-oxidant activity of the synthesized compounds (3a-3n) from $DPPH^+$ and $ABTS^+$ assays, the Ascorbic acid and Gallic acid used as standard drugs. In the DPPH+ assay, the findings indicate that all tested compounds (3a-3n) demonstrate the IC_{50} values range from 21.69 ± 0.66 µg/mL for compound 3c to 32.43 ± 1.89 µg/mL for compound 3n. Notably, compounds 3c, 3a, and 3i exhibit comparatively higher antioxidant activity, with IC_{50} values below 28 µg/mL. For reference, Ascorbic acid shows an IC_{50} value of 16.94 ± 2.2 µg/mL. Whereas for $ABTS^+$ the IC_{50} values vary from 15.6 ± 1.8 µg/mL for compound 3l to 35.82 ± 2.6 µg/mL for compound 3i. Compounds 3l, 3e, and 3d demonstrate notably higher antioxidant activity, exhibiting IC_{50} values of less than 25 µg/mL. For reference, gallic acid has an IC_{50} value of 16.2 ± 0.67 µg/mL. (Table 2) (Figure 5a-b).

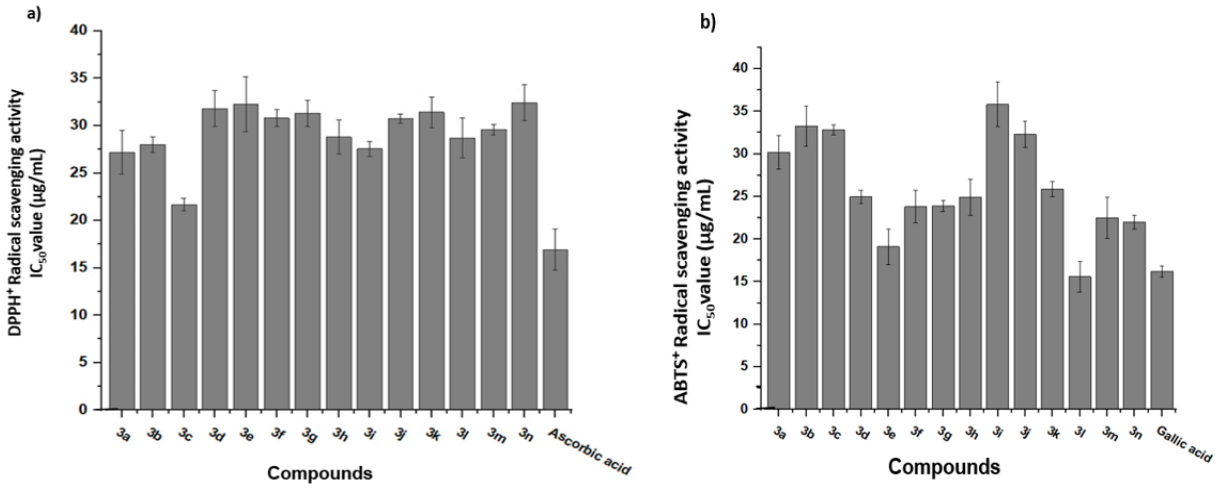

Figure 5a-b. IC_{50} values of a) $DPPH^+$ and b) $ABTS^+$ radical scavenging activity of triazole compounds. Values are mean ± SD of three independent experiments.

3.2.2. MTT Assay

In this study, the cytotoxic activity of tested 1,2,3-triazoles hybrids was evaluated against a human breast tumor cell line MCF-7 and Cisplatin used as reference drug.[62] The results were obtained after analysis treatment of the synthesized compounds, then calculated IC_{50} values and are presented in (Table 3).

The obtained cell viability results that most of the synthesized compounds displayed a lower IC_{50} value against MCF-7 cell line at different concentrations ranging from 2.5 µg/mL to 50 µg/mL. The findings indicate that all tested compounds (3a-3n) demonstrate antiproliferative effects on MCF-7 cancer cell line, with IC_{50} values varying from 14.08 ± 0.6 µg/mL for compound 3b to 32.4 ± 2.2 µg/mL for compound 3e. Compounds indicates electron-withdrawing groups, like 3b and 3d, are exhibit more potent antiproliferative effects (IC_{50}-14.08 ±0.6 µg/mL, 14.3 ±0.8 µg/mL). In contrast, compounds with electron-donating groups, such as 3e and 3f are to demonstrate less antiproliferative activity (IC_{50}-32.4 ±2.2 µg/mL, 25.2 ±0.65 µg/mL). Additionally, the inclusion of halogen atoms like F, Cl, and Br appears to boost antiproliferative activity. Furthermore, the location of the substituent on the phenyl ring seems to play a significant role in modulating antiproliferative effects. Cisplatin, a widely recognized anticancer agent, has an IC_{50} value of 21.13 ± 1.6 µg/mL. Various compounds, specifically 3b, 3d, and 3m, demonstrate greater antiproliferative efficacy compared to Cisplatin (Figure 6a-b).

Table 3. The IC_{50} values are mean ± SD from three replicates and represent the inhibitory activity of the tested compounds against tumor cell (MCF-7) lines.

Entry	Compounds	Functional Group	IC_{50} (µg/mL)
1	**3a**	H	15.82 ± 0.4
2	**3b**	4F	14.08 ±0.6
3	**3c**	3Cl	23.7 ±1.86
4	**3d**	2, 6- Di CH_3	14.3 ±0.8
5	**3e**	2 F	32.4 ±2.2
6	**3f**	4 Cl	25.2 ±0.65
7	**3g**	2 Cl	27.7 ±1.6
8	**3h**	4- OMe	22.5 ±1.5
9	**3i**	3, 5- Di Cl	19.7 ±0.88
10	**3j**	4 CH_3	21.85 ±1.6
11	**3k**	4 Br	21.26 ±1.2
12	**3l**	3 CH_3	22.7 ±1.8
13	**3m**	2, 4 Di CH_3	18.12 ±0.86
14	**3n**	2 CH_3	27.75 ±1.7
15	Cisplatin	-	21.13 ±1.6

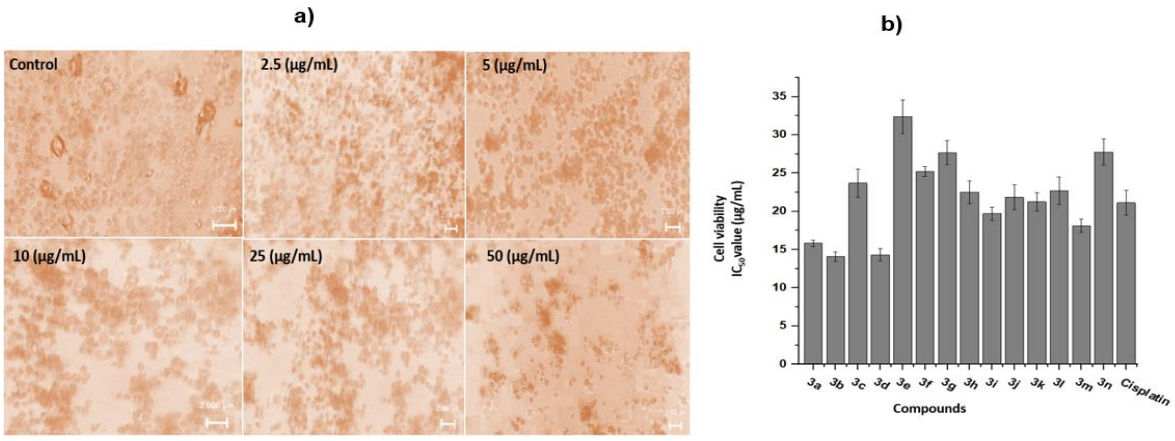

Figure 6a-b. The MTT assay was conducted for synthesized compounds. Cells were treated to compounds (3a–3n) at varying concentrations for 24 hours, cell viability was assessed. The results are presented as the mean ± SD from three independent experiments. **a).** Cytotoxicity test using MTT assay against different concentrations on MCF-7 cell lines. **b).** Representation of IC_{50} values of synthesized compounds along with reference drug Cisplatin.

3.3. In-silico Studies

3.3.1. Prediction of Compounds Pharmacophore and AMDET Properties by Using in silico Studies

ADMET stands for Absorption, Distribution, Metabolism, Excretion, and Toxicity. These properties are crucial in evaluating the pharmacokinetics (PK) and pharmacodynamics (PD) of a drug candidate (Table 4). An ideal drug candidate must exhibit suitable ADMET characteristics at therapeutic concentrations while also demonstrating efficacy against the intended therapeutic target. The results indicate Compounds 3a-3n show good oral bioavailability (high GI absorption), 3i and 3j show potential for CNS activity (BBB permeability) and transdermal delivery (high skin permeation). Several compounds show CYP inhibition activity, which may lead to drug-drug interactions. Cisplatin shows poor oral bioavailability and low skin permeation[63].

Table 4. ADMET analysis of 1,2,3 triazoles synthesized compounds

Compounds	GI absorption	BBB permeant	P-gp substrate	CYP1A2 inhibitor	CYP2C19 inhibitor	CYP2C9 inhibitor	CYP2D6 inhibitor	CYP3A4 inhibitor	Log K_p (skin permeation)
3a	High	No	No	No	No	No	No	No	-7.09cm/s
3b	High	No	No	No	No	No	No	No	-7.13cm/s
3c	High	No	No	Yes	No	No	No	No	-6.85 cm/s
3d	High	No	No	Yes	No	No	No	No	-6.74 cm/s
3e	High	No	No	Yes	No	No	No	No	-7.13 cm/s
3f	High	No	No	Yes	No	No	No	No	-6.85 cm/s
3g	High	No	No	Yes	Yes	No	No	No	-6.85 cm/s
3h	High	No	No	No	No	No	No	No	-7.29 cm/s
3i	High	Yes	No	Yes	Yes	No	No	No	-6.61 cm/s
3j	High	Yes	No	Yes	Yes	No	No	No	-6.91 cm/s
3k	High	No	No	Yes	Yes	No	No	No	-7.08 cm/s
3l	High	No	No	No	No	No	No	No	-6.91 cm/s
3m	High	No	No	No	No	No	No	No	-6.74 cm/s
3n	High	No	No	No	No	No	No	No	-6.91 cm/s
Cisplatin	Low	No	No	No	No	No	No	No	-2.50 cm/s

The Lipinski rule, which is based on molecular weight, AlogP, number of rotatable bonds, number of H-bond donors, and number of H-bond acceptors. To estimate 1,2,3 Triazoles synthesized compounds drug-like qualities using reference drugs represented in (Table 5). The examination of molecular characteristics offers important understanding regarding the possible pharmacokinetic and pharmacodynamics attributes of the compounds.

Table 5. Pharmacophore analysis of 1,2,3 triazoles synthesized compounds

Compound	Molecular Wight (g/mol)	miLogP	natoms	nON	nOHNH	nrotb
3a	258.28	1.02	19	6	1	4
3b	276.27	1.18	20	6	1	4
3c	292.72	1.67	20	6	1	4
3d	286.33	0.88	21	6	1	4
3e	276.27	1.13	20	6	1	4
3f	292.72	1.69	20	6	1	4
3g	292.72	1.65	20	6	1	4
3h	288.30	1.07	21	7	1	5
3i	327.16	2.30	21	6	1	4
3j	272.30	1.46	20	6	1	4
3k	337.17	1.82	20	6	1	4
3l	272.30	1.44	20	6	1	4
3m	286.33	1.84	21	6	1	4
3n	272.30	1.42	20	6	1	4
Cisplatin	300.05	2.0	6	1	2	0

3.3.2. In-silico Bioactivity Study

The biological activity score of synthetic compounds was also evaluated using the molinspiration cheminformatics server application (Molinspiration Cheminformatics). Understanding the active site or binding mechanism through biological activity studies is necessary to comprehend how chemicals behave biologically represented in (Table 6).

Table 6. Bioactivity score of 1,2,3 Triazoles synthesized compounds with reference drugs

Compound	GPCR ligand	Ion channel modulator	Kinase inhibitor	Nuclear receptor ligand	Protease inhibitor	Enzyme inhibitor
3a	-0.41	-0.57	-0.55	-0.93	-0.63	-0.40
3b	-0.34	-0.56	-0.44	-0.80	-0.58	-0.39
3c	-0.36	-0.56	-0.49	-0.87	-0.64	-0.44
3d	-0.35	-0.58	-0.46	-0.78	-0.62	-0.36
3e	-0.40	-0.55	-0.43	-0.86	-0.55	-0.39
3f	-0.35	-0.55	-0.50	-0.85	-0.61	-0.41
3g	-0.38	-0.57	-0.46	-0.91	-0.68	-0.45
3h	-0.35	-0.61	-0.46	-0.77	-0.55	-0.40
3i	-0.29	-0.51	-0.43	-0.77	-0.56	-0.40
3j	-0.38	-0.61	-0.52	-0.86	-0.60	-0.42
3k	-0.47	-0.64	-0.53	-0.97	-0.70	-0.46
3l	-0.39	-0.63	-0.52	-0.86	-0.61	-0.44
3m	-0.36	-0.61	-0.48	-0.76	-0.57	-0.43
3n	-0.40	-0.60	-0.51	-0.84	-0.62	-0.43
Cisplatin	-3.73	-3.68	-3.74	-3.53	-3.75	-3.70

The biological validation of selected target protein analysis by BLAST (Basic Local Alignment Search Tool) algorithm and software are employed for the comparison of primary biological sequence data. This tool facilitates the comparison of protein or nucleotide sequences against sequence databases, identifying specific regions of similarity between the query sequences and the entries within the database.[64] The program assesses the statistical significance of these alignments. BLAST facilitates rapid alignment and comparison of a query DNA sequence against a sequence database. It simplifies the process of identifying evolutionary and functional relationships among sequences (Table 7).

Table 7. The identification of target gene by Blastp analysis

Sl.no	Target protein	length	Sequence ID	% of identify	Sequence coverage	Total score
1.	HIF-1α	805	XP_047275238.1	100	16-805	4295
		790	NP_001257436.1	100	1-790	4294
		790	ACN87239.1	100	1-790	4293
2.	HER2	212	NP_000591.1	100	1-212	1123
		211	AFF18412.1	99	1-211	1104
		185	AAB30962.1	100	1-185	984

Table 8. The identification of active amino acids target proteins

Sl.no	Protein name	Protein code	Area (SA) A^2	Volume (SA) A^3	Active amino acids
1.	HIF-1α	1H2N	285.017	143.167	Lys 98, Ser 99, Pro 100, Cys 101, Gln 102, Gln14, Glu 104, Asn294, Trp 114, Tyr 115 Asn205. Arg238, Leu188.
2.	HER2	3PP0	63.542	38.585	Gln 75, Arg 179, Phe 74, Ser783, Thr862, Leu852, Val734, Leu852.

The synthesized compounds have done prediction of active amino acid by CastP calculation server. The examination of protein structures offers critical insights into possible binding sites and active amino acids. This knowledge can inform subsequent research efforts, including molecular docking and virtual screening, aimed at discovering potential inhibitors (Table 8).

3.2.3. Molecular Docking Analysis

The homology modelled proteins like HIF-1α and HER2 are used for docking. Gasteiger charges and polar hydrogens were given to the macromolecules before to docking, AutoDock Vina 4.2 were used to add partial change to integrate nonpolar and polar hydrogen atoms. Rotatable bonds were identified and non-polar hydrogen atoms were combined with polar hydrogen atoms for synthesized compounds in addition to conventional pharmaceuticals for comparison. Grid maps and rigid or flexible macromolecules are produced by setting the grid dimension to 40 × 40 × 40 points and spacing to 0.421Å to facilitate ligand binding. The grid centre was chosen with dimensions of x = 25.665, y = 25.128, and z = 23.187. The total binding site energy for each grid is determined using an equilibrated energy distribution for the amino acid composition. The configuration file is produced as a text file that can be run in AutoDock Vina to assess the target and ligand proteins' ability to bind. Subsequently, the implementation of a grid file facilitated the generation of a ligand log file, which was utilized to execute the docking score for the application known as Cygwin. Confirmation was achieved following an exhaustiveness score of 10. The results were derived from the PyMOL analysis of the protein-ligand complex, focusing on the binding energy and the interactions of hydrogen bonds established by the active amino acids (Table 9 and 10). The interactions between the ligand and protein were additionally illustrated in both two-dimensional and three-dimensional formats using the BIOVIA Discovery Studio Visualizer.[65]

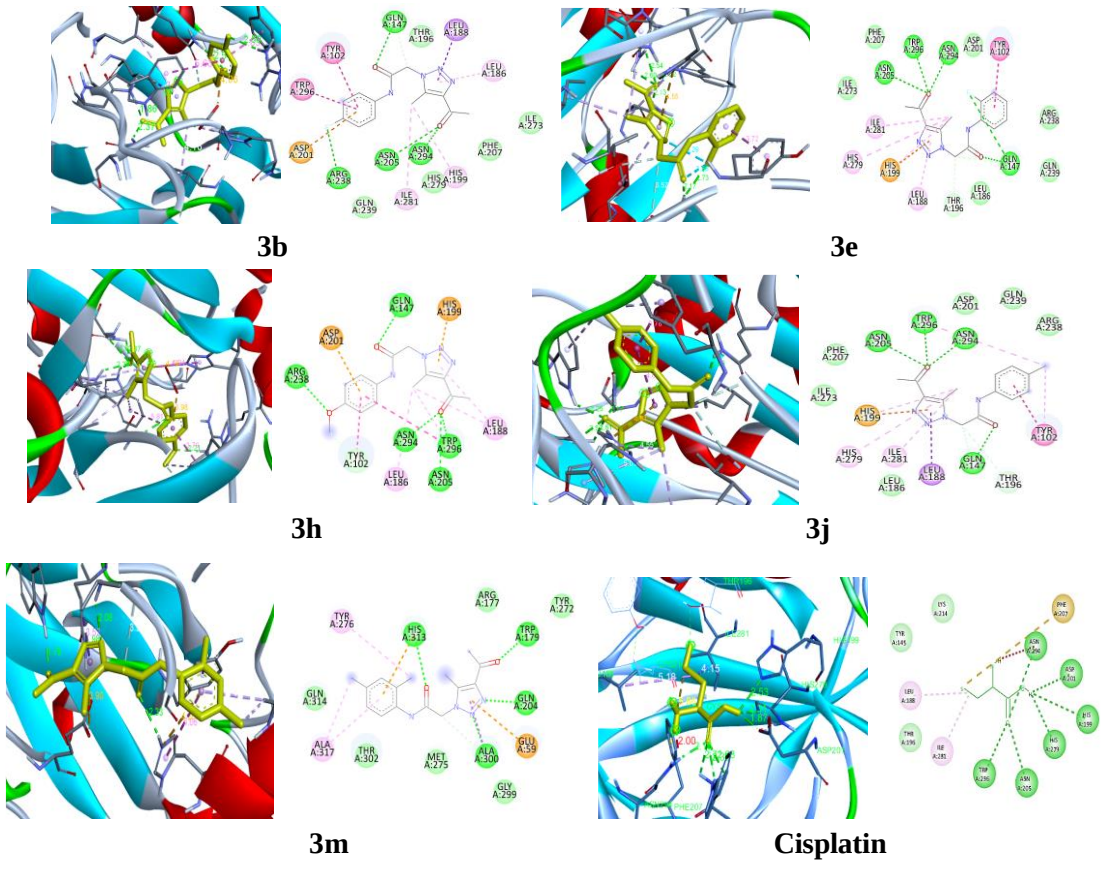

Figure 7. 2D and 3D poses of synthesized compounds and reference drug with their binding complex of protein HIF-1α.

Table 9. Binding affinity of HIF-1α against synthesized compounds and reference against selected protein

Compounds	Binding affinity (kcal/mol)	Type of bond	Amino acids	Bond length (Å)
3a	-7.5	H-bond	Ser184, Asn294	2.04, 2.22
		Pi-sigma	Leu188	3.78
		Pi-alkyl	Leu186	4.42
3b	-7.4	H-bond	Asn205. Arg238, Gln147,	1.86, 2.27, 2.50, 2.54,
		Pi-sigma	Asn294	3.75
		Pi-alkyl	Leu188	5.44
			Ile281	
3c	-7.5	H-bond	Gln147, Tyr93	2.11, 2.68
		Pi-alkyl	Ile281	3.08
3d	-7.5	H-bond	Asn294, Asn205, Trp296	2.38, 2.40, 2.61
		Pi-alkyl	Leu186	4.41
		Pi-alkyl	Leu188	4.63
3e	-7.8	H-bond	Gln147, Asn205, Trp296,	2.17, 2.22, 2.54, 2.60
		Pi-alkyl	Asn294	4.18
			Leu188	
3f	-7.6	H-bond	Gln314	2.24
		Pi-alkyl	Arg177	4.09
3g	-7.0	H-bond	Gln147	2.26
		Pi-alkyl	Leu186	4.39
		Pi-alkyl	His199	4.50
3h	-7.2	H-bond	Gln147, Arg238, Asn294,	2.21, 2.21, 2.39, 2.47,
			Asn205, Trp296	2.82
		Pi-alkyl	Leu186	4.49
3i	-7.4	H-bond	Gln147, His279	2.29, 2.80
		Pi-sigma	Trp296, Leu186	3.55, 3.95
3j	-8.1	H-bond	Gln147, Asn205, Trp296,	2.06, 2.17, 2.25, 2.53
		Pi-sigma	Asn294	4.55
		Pi-alkyl	Leu188	4.32, 4.55
			His279, Ile4.55	
3k	-7.3	H-bond	Gln147	2.35
		Pi-alkyl	Leu188	4.25
3l	-7.7	H-bond	Arg238	2.14
		Pi-alkyl	Ile281, Leu188	3.66, 4.98
3m	-7.7	H-bond	Trp179, Gln204, Ala300,	1.79, 1.98, 2.08, 2.33
		Pi-alkyl	His313	4.08, 5.05
			Try276, Ala317	
3n	-7.3	H-bond	His199, Asn294, His279	2.32, 2.58, 2.74
		Pi-sigma	Leu186, Tyr102	3.59, 5.11
Cisplatin	-3.9	H-bond	Asn294, Asp201, His199, Trp296	2.31, 2.53, 1.87, 2.68

The docking analysis shows the results of synthesized compounds **(3a-3n)** with HIF-1α showed the binding affinity ranging from -8.1 kcal/mol to -7.0 kcal/mol. The first lead compound **3h** exhibits the binding affinity of -7.2 kcal/mol which represents the five hydrogen bonds with following amino acids Gln147, Arg238, Asn294, Asn205 and Trp296 (bond length 2.21Å, 2.21Å, 2.39Å, 2.47Å and 2.82Å). The second lead compound **3j** exhibits a good binding affinity of -8.1kcal/mol which represents the 4 hydrogen bonds with following amino acids Gln147, Asn205, Trp296 and Asn294 (bond length 2.06Å, 2.17Å, 2.25Å and 2.53Å). The third lead compound **3m** is exhibits the good binding affinity of

-7.7 kcal/mol which represents the four hydrogen bonds with the following amino acids Trp179, Gln204, Ala300, and His313 (bond length 1.79Å, 1.98Å, 2.08Å and 2.33Å). The fourth lead compound **3e** ~~is~~ exhibits a good binding affinity of -7.8 kcal/mol which represents the four hydrogen bonds with following amino acids Gln14, Asn205, Trp296 and Asn294 (bond length 2.17Å, 2.22Å, 2.54Å and 2.60Å). The fifth lead compound **3b** exhibits a good binding affinity of -7.4 kcal/mol which represents the four hydrogen bonds with following amino acids Asn205. Arg238, Gln147and Asn294 (bond length 1.86Å, 2.27Å, 2.50Å and 2.54Å). The reference drug Cisplatin is also showing the binding affinity of -3.9 kcal/mol which represents the four hydrogen bonds with following amino acids Asn294, Asp201, His199 and Trp296 (bond length 2.31Å, 2.53Å, 1.87Å and 2.68Å). The present docking analysis represents the synthesized compounds like (3a-3n) exhibiting the anticancer activity with the reference drug (Figure 7).

Table 10. Binding affinity of HER2 against synthesized compounds and reference against selected protein

Compound	Binding affinity (kcal/mol)	Type of bond	Amino acid	Bond length
3a	-8.8	H-bond	Ser783	3.20
		Pi-sigma	Leu852	3.58
3b	-8.8	H-bond	Ser783	3.20
		Pi-sigma	Leu852	3.68
3c	-9.4	H-bond	Ser783	2.97
		Pi-sigma	Val734	3.60
		Pi-alkyl	Ala751	4.84
3d	-10.0	Pi-sigma	Val734	3.71
		Pi-alkyl	Lys753	4.56
3e	-8.8	H-bond	Ser783, Thr862	2.29, 2.92
		Pi-alkyl	Leu852, Val734	4.55, 5.02
3f	-9.0	H-bond	Ser783	3.03
		Pi-sigma	Leu852	3.67
		Pi-alkyl	Val734, Ala751	4.69, 4.82
3g	-9.0	H-bond	Asp653	2.95
		Pi-sigma	Thr862	3.75
		Pi-alkyl	Leu785, Leu796	4.80, 5.44
3h	-8.9	H-bond	Ser783,	2.98
		Pi-sigma	Val734, Leu852	3.92, 3.92
		Pi-alkyl	Ala751	4.30
3i	-9.1	H-bond	Ser783	3.01
		Pi-sigma	Val734, Leu852	3.87, 3.96
		Pi-alkyl	Leu800	4.85
3j	-9.2	H-bond	Ser783	2.87
		Pi-sigma	Leu852	3.69
		Pi-alkyl	Ala751	3.79
3k	-9.2	H-bond	Ser783	3.02
		Pi-sigma	Leu852	3.68
		Pi-alkyl	Ala751, Val734	4.41, 4.63
3l	-9.5	H-bond	Ser783, Thr862	2.22, 2.56
		Pi-sigma	Val734	3.88
		Pi-alkyl	Lys753	3.83
3m	-9.2	H-bond	Ser783	2.55
		Pi-sigma	Val734	3.73
		Pi-alkyl	Leu852	4.46
3n	-9.4	Pi-sigma	Val734	3.70
		Pi-alkyl	Leu796, Lys752	4.80, 5.42
Cisplatin	-4.2	H-bond	Asn294, Asp201, His199,Asn205	2.71, 2.38, 2.68, 2.16

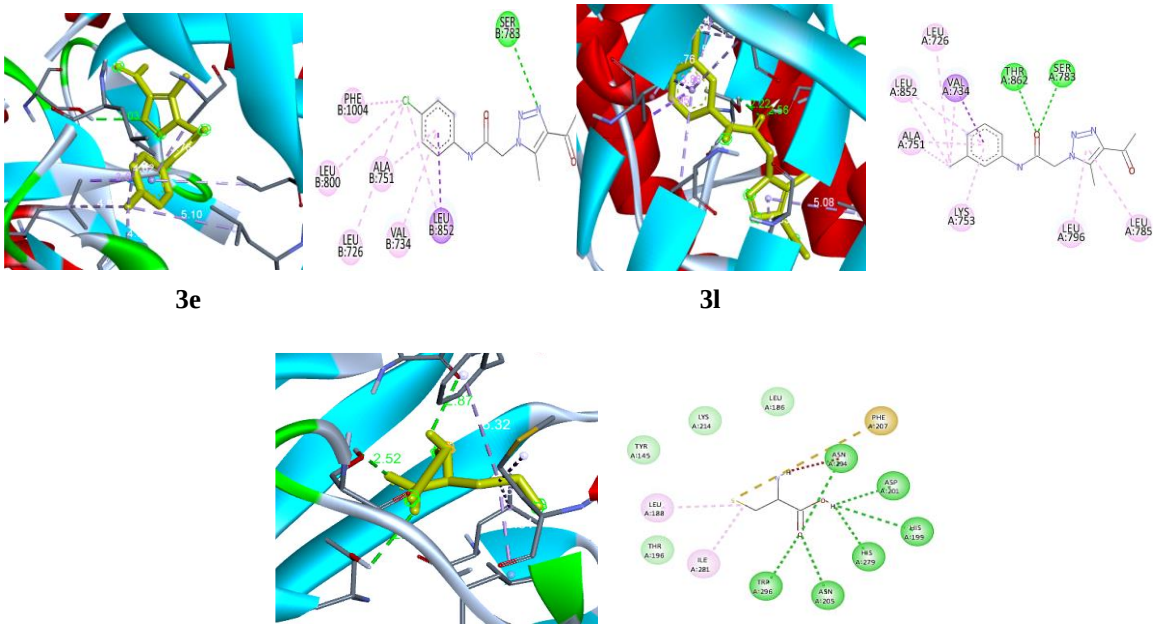

Figure 8. 2D and 3D poses of synthesized compounds and reference drug with their binding complex of protein HER2.

The docking analysis shows the results of selected synthesized compounds with HER2 have a higher binding affinity ranging from -10.0 kcal/mol to -8.8 kcal/mol. The first lead compound **3l** exhibits the binding affinity of -9.5 kcal/mol which represents the two hydrogen bonds with following amino acids Ser783 and Thr862 (bond length 2.22 Å and 2.56Å). The second lead compound **3e** exhibits a good binding affinity of -8.8 kcal/mol which represents the two hydrogen bonds with following amino acids Ser783 and Thr862 (bond length 2.29 Å and 2.92Å). The reference drug Cisplatin is also showing the binding affinity of -4.2 kcal/mol which represents the five hydrogen bonds with following amino acids Asn294, Asp201, His199 and Asn205 (bond length 2.71Å, 2.38Å, 2.68Å and 2.16Å) (Figure 8).

4. Conclusion

To sum up, this study shows the development of an efficient green and one pot procedure for the synthesis of substituted 2-(4-acetyl-5-methyl-1H-1,2,3-triazol-1-yl)-N-phenylacetamide from 2-chloro-N-phenylacetamide using sodium azide, acetyl acetone and K_2CO_3 in ethanol: water medium in a reflux system. The reaction proceeds through nucleophilic substitution of halide by sodium azide to form 2-azido-N-phenylacetamide, which was then converted into the desired product by cyclization with acetyl acetone, both electron-donating and electron-withdrawing substituents on the aromatic ring of amide were given excellent yields. The synthesized compounds were evaluated for their free radical scavenging activities using *in vitro* assays, such as $DPPH^+$ and $ABTS^+$. The results have showed that these compounds exhibited notable scavenging potential, with inhibition rates compared to standard antioxidants like Ascorbic acid and Gallic acid. Additionally, the anticancer effects of the newly synthesized compounds (**3a-3n**) were tested against the MCF-7 human breast cancer cell line using MTT assays, with cisplatin serving as the positive control. Most of the evaluated compounds displayed good to moderate IC_{50} values, among all, compounds **3b, 3d, 3a, 3m** and **3i** exhibited more potent activity. Molecular docking studies reveal the synthesized compounds showed good binding affinity with a good number of hydrogen bonds with active amino residues of cancer target proteins like HIF-1α and HER2 as compared to the reference drug Cisplatin.

Acknowledgement

Lakshmi Basavegowda gratefully acknowledges the analytical support provided by the Sophisticated Central Instrumentation Facility of IIT Dharwad. A. M. M. Mallikarjunaswamy expresses gratitude to REVA University for the research fellowship and funding.

Competing Interests

The authors declare no conflict of interest either of a financial or personal nature.

Supporting Information

Supporting information accompanies this paper on http://www.acgpubs.org/journal/organic-communications

ORCID

Aiyagala M. M. Mallikarjunaswamy: 0000-0002-7997-4216
Kuruvalli Gouthami: 0000-0003-0077-6995
Subhasish Maity: 0009-0009-1817-4168
Vaddi Damodara Reddy: 0000-0002-4441-0859
Lakshmi Basavegowda: 0000-0002-3802-3166

References

[1] Bonandi, E.; Christodoulou, M. S.; Fumagalli, G.; Perdicchia, D.; Rastell, G.; Passarella, D. The 1, 2, 3-triazole ring as a bioisostere in medicinal chemistry. *Drug. Discov. Today.* **2017**, *22*, 1572-1581.
[2] Bozorov, K.; Zhao, J.; Aisa, H. A. 1, 2, 3-Triazole-containing hybrids as leads in medicinal chemistry: A recent overview. *Bioorg. Med. Chem.* **2019**, *27*, 3511-3531.
[3] Lal, K.; Yadav, P. Recent advancements in 1, 4-disubstituted 1H-1, 2, 3-triazoles as potential anticancer agents. Anti-Cancer Agents in Medicinal Chemistry. *Curr. Med. Chem. Anticancer Agents.* **2018**, *18*, 21-37.
[4] Akhtar, J.; Khan, A. A.; Ali, Z.; Haider, R.; Yar, M. S. Structure-activity relationship (SAR) study and design strategies of nitrogen-containing heterocyclic moieties for their anticancer activities. *Eur. J. Med. Chem.* **2017**, *125*, 143-189.
[5] Liang, T.; Sun, X.; Li, W.; Hou, G.; Gao, F. 1, 2, 3-Triazole-containing compounds as anti–lung cancer agents: Current developments, mechanisms of action, and structure–activity relationship. *Front. Pharmacol.* **2021**, *12*, 661173.
[6] Slavova, K. I.; Todorov, L. T.; Belskaya, N. P.; Palafox, M. A.; Kostova, I. P. Developments in the application of 1, 2, 3-triazoles in cancer treatment. Recent Patents on Anti-Cancer Drug Discovery. **2020**, *15*, 92-112.
[7] Castelli, V.; Derita, G.; Lopez, N. Novel antifungal agents: a patent review (2013-present). Expert Opinion on Therapeutic Patents. **2017**, *27*, 415-426.
[8] Syed, S.; Alam, M. M.; Mulakayala, N.; Mulakayala, C.; Vanaja, G.; Kalle, A. M.; Pallu, R. R.; Alam, M. S. Synthesis of novel 2-mercapto benzothiazole and 1, 2, 3-triazole based bisheterocycles: Their anti-inflammatory and anti-nociceptive activities. *Eur. J. Med. Chem.* **2012**, *49*, 324-333.
[9] Ali, Y.; Alam, M. S.; Hamid, H.; Husain, A.; Bano, S.; Dhulap, A.; Kharbanda, C.; Nazreen, S.; Haider, S. Design, synthesis and biological evaluation of piperic acid triazolyl derivatives as potent anti-inflammatory agents. *Eur. J. Med. Chem.* **2015**, *92*, 490-500.
[10] Keri, R. S.; Patil, S. A.; Budagumpi, S.; Nagaraja, B. M. Triazole: a promising antitubercular agent. *Chem. Biol. Drug. Des.* **2015**, *86*, 410-423.
[11] Tian, Y.; Liu, Z.; Liu, J.; Huang, B.; Kang, D.; Zhang, H.; De Clercq, E.; Daelemans, D.; Pannecouque, C.; Lee, K. H.; Chen, C. H. Targeting the entrance channel of NNIBP: Discovery of diarylnicotinamide 1, 4-disubstituted 1, 2, 3-triazoles as novel HIV-1 NNRTIs with high potency against wild-type and E138K mutant virus. *Eur. J. Med. Chem.* **2018**, *151*, 339-350.

[12] Kaoukabi, H.; Kabri, Y.; Curti, C.; Taourirte, M.; Rodriguez-Ubis, J. C.; Snoeck, R.; Andrei, G.; Vanelle, P.; & Lazrek, H. B. Dihydropyrimidinone/1, 2, 3-triazole hybrid molecules: Synthesis and anti-varicella-zoster virus (VZV) evaluation. *Eur. J. Med. Chem.* **2018**, *155*, 772-781.

[13] Ahmed, F.; Xiong, H. Recent developments in 1, 2, 3-triazole-based chemosensors. *Dyes Pigment.* **2021**, *185*, 108905.

[14] Trost, B. M.; Fleming, I. (Eds.). Comprehensive organic synthesis: selectivity, strategy, and efficiency in modern organic chemistry (Vol. 8). Elsevier. **1991**.

[15] Feng, S. B.; Li, F. S.; Zhao, X. Y.; Qian, Y. D.; Fe, T.; Yin, P.; Pang, S. P. Comparative study on 1, 2, 3-triazole based azo-and triazene-bridged high-nitrogen energetic materials. *Energ. Mater. Front.* **2021**, *2*, 125-130.

[16] Ashwini, N.; Garg, M.; Mohan, C. D.; Fuchs, J. E.; Rangappa, S.; Anusha, S.; Swaroop, T. R.; Rakesh, K. S.; Kanojia, D.; Madan, V.; Bender, A. Synthesis of 1, 2-benzisoxazole tethered 1, 2, 3-triazoles that exhibit anticancer activity in acute myeloid leukemia cell lines by inhibiting histone deacetylases, and inducing p21 and tubulin acetylation. *Bioorg. Med. Chem.* **2015**, *23*, 6157-6165.

[17] Stefely, J. A.; Palchaudhuri, R.; Miller, P. A.; Peterson, R. J.; Moraski, G. C.; Hergenrother, P. J.; & Miller, M. J. N-((1-benzyl-1 H-1, 2, 3-triazol-4-yl) methyl) arylamide as a new scaffold that provides rapid access to antimicrotubule agents: Synthesis and evaluation of antiproliferative activity against select cancer cell lines. *J. Med. Chem.* **2010**, *53*, 3389-3395.

[18] Grymel, M.; Pastuch-Gawołe, G.; Lalik, A.; Zawojak, M.; Boczek, S.; Krawczyk, M.; & Erfurt, K. Glycoconjugation of betulin derivatives using copper-catalyzed 1, 3-dipolar azido-alkyne cycloaddition reaction and a preliminary assay of cytotoxicity of the obtained compounds. *Molecules* **2020**, *25*, 6019.

[19] Luan, T.; Quan, Z.; Fang, Y.; Yang, H. Design, Synthesis and Antiproliferative Activity of Chrysin Derivatives Bearing Triazole Moieties. *Chin. J. Org. Chem.* **2020**, *40*, 440–46.

[20] Gholampour, M.; Ranjbar, S.; Edraki, N.; Mohabbati, M.; Firuzi, O.; Khoshneviszadeh, M. Click chemistry-assisted synthesis of novel aminonaphthoquinone-1, 2, 3-triazole hybrids and investigation of their cytotoxicity and cancer cell cycle alterations. *Bioorg. Chem.* **2019**, *88*, 102967.

[21] Padwa, A. I.; Pearson, W. H. Synthesis applications of 1, 3-dipolar cycloaddition chemistry. Wiley, New York. **1984**.

[22] Xie, F.; Sivakumar, K.; Zeng, Q.; Bruckman, M. A.; Hodges, B.; Wang, Q. A fluorogenic 'click' reaction of azidoanthracene derivatives. *Tetrahedron.* **2008**, *64*, 13, 2906-2914.

[23] Sivakumar, K.; Xie, F.; Cash, B. M.; Long, S.; Barnhill, H. N.; Wang, Q. A fluorogenic 1, 3-dipolar cycloaddition reaction of 3-azidocoumarins and acetylenes. *Org. Lett.* **2004**, *6*, 4603-4606.

[24] Kamijo, S.; Jin, T.; Huo, Z.; Yamamoto, Y. A one-pot procedure for the regiocontrolled synthesis of allyltriazoles via the Pd−Cu bimetallic catalyzed three-component coupling reaction of nonactivated terminal alkynes, allyl carbonate, and trimethylsilyl azide. *J. Org. Chem.* **2004**, *69*, 2386-2393.

[25] Jin, X.; Wang, A.; Cao, H.; Zhang, S.; Wang, L.; Zheng, X.; Zheng, X. A new efficient method for the preparation of intermediate aromatic ketones by Friedel–Crafts acylation. *Res. Chem. Intermed.* **2018**, *44*, 5521-5530.

[26] Janreddy, D.; Kavala, V.; Kuo, C. W.; Chen, W. C.; Ramesh, C.; Kotipalli, T.; Kuo, T. S.; Chen, M. L.; He, C. H.; Yao, C. F. Copper (I)-Catalyzed Aerobic Oxidative Azide–Alkene Cyclo-addition: An Efficient Synthesis of Substituted 1, 2, 3-Triazoles. *Adv. Synth. Catal.* **2013**, *355*, 2918-2927.

[27] Romeiro, G. A.; Pereira, L. O.; de Souza, M. C. B.; Ferreira, V. F.; Cunha, A. C. A new and efficient procedure for preparing 1, 2, 3-triazoles. *Tetrahedron. Lett.* **1997**, *38*, 5103-5106.

[28] Boyer, J.; Mack, C.; Goebel, N.; & Morgan Jr, L. Reactions of sodium phenylacetylide and sodium alkoxide with tosyl and mesyl azides. *J. Org. Chem.* **1958**, *23*, 1051-1053.

[29] Artyushin, O. I.; Vorob'eva, D. V.; Vasil'eva, T. P.; Osipov, S. N.; Röschenthaler, G. V.; Odinets, I. L. Facile synthesis of phosphorylated azides in ionic liquids and their use in the preparation of 1, 2, 3-triazoles. *Heteroat. Chem.* **2008**, *19*, 293-300.

[30] Tanaka, Y.; Miller, S. I. Synthesis and nucleophilic properties of 4-aryl-5-triphenylphosphonium-1, 2, 3-triazole ylides or 4-aryl-1, 2, 3-triazol-5-yltriphenylphosphoranes. *J. Org. Chem.* **1973**, *38*, 2708-2712.

[31] Peng, W.; & Zhu, S. Efficient synthesis of 5-fluoroalkylated 1H-1, 2, 3-triazoles and application of the bromodifluoromethylated triazole to the synthesis of novel bicyclic gem-difluorinated 1H-pyrano [3, 4-d][1, 2, 3]-triazol-4-one compounds. *Tetrahedron.* **2003**, *59*, 4395-4404.

[32] Zanirato, P. The role of the carbonyl group in the intermolecular 1, 3-cycloaddition of azido (2-heteroaryl) methanones with activated olefins. *J. Chem. Soc. Perkin. Trans 1.* **2002**, *12*, 1420-1425.

[33] Adamo, I.; Benedetti, F.; Berti, F.; Nardin, G.; & Norbedo, S. Unexpected 1, 2, 3-triazole formation in the reaction of diethylaluminum azide with α′-amino-α, β-unsaturated ketones. *Tetrahedron. Lett.* **2003**, *44*, 9095-9097.

[34] Tanaka, Y.; Miller, S. I. 2H-1, 2, 3-Triazoles from the ethyl nitrocinnamates. *J. Org. Chem.* **1972**, *37*, 3370-3372.
[35] Garanti, L.; Molteni, G. MeOPEG-bounded azide cycloadditions to alkynyl dipolarophiles. *Tetrahedron. Lett.* **2003**, *44*, 1133-1135.
[36] Freeze, S.; Norris, P. Synthesis of carbohydrate-derived 1, 2, 3-triazoles using 1, 3-dipolar cycloaddition on a soluble polymer support. *Heterocycles*. **1999**, *8*, 1807-1817.
[37] Moore, M.; Norris, P. Dipolar cycloaddition reactions on a soluble polymer-supported dipolarophile: Synthesis of sugar-derived triazoles. *Tetrahedron. Lett*. **1998**, *39*, 7027-7030.
[38] Zaragoza, F.; Petersen, S. V. Solid-phase synthesis of substituted 1, 2, 3-triazoles. *Tetrahedron*. **1996**, *52*, 10823-10826.
[39] Wang, Z. X.; Qin, H. L. Regioselective synthesis of 1, 2, 3-triazole derivatives via 1, 3-dipolar cycloaddition reactions in water. *Chem. Commun*. **2003**, *19*, 2450-2451.
[40] Li, Z.; Seo, T. S.; & Ju, J. 1, 3-Dipolar cycloaddition of azides with electron-deficient alkynes under mild condition in water. *Tetrahedron. Lett*. **2004**, *45*, 3143-3146.
[41] Rostovtsev, V. V.; Green, L. G.; Fokin, V. V.; Sharpless, K. B. A stepwise Huisgen cycloaddition process: copper (I)-catalyzed regioselective "ligation" of azides and terminal alkynes. *Angew. Chem*. **2002**, *114*, 2708-2711.
[42] Chan, T. R.; Hilgraf, R.; Sharpless, K. B.; Fokin, V. V. Polytriazoles as copper (I)-stabilizing ligands in catalysis. *Org. Lett*. **2004**, *6*, 2853-2855.
[43] Pachón, L. D.; van Maarseveen, J. H.; Rothenberg, G. Click chemistry: Copper clusters catalyse the cycloaddition of azides with terminal alkynes. *Adv. Synth. Catal*. **2005**, *347*, 811-815.
[44] Tornøe, C. W.; Christensen, C.; Meldal, M. Peptidotriazoles on solid phase: [1, 2, 3]-triazoles by regiospecific copper (I)-catalyzed 1, 3-dipolar cycloadditions of terminal alkynes to azides. *J. Org. Chem*. **2002**, *67*, 3057-3064.
[45] Fazio, F.; Bryan, M. C.; Blixt, O.; Paulson, J. C.; Wong, C. H. Synthesis of sugar arrays in microtiter plate. *J. Am. Chem. Soc*. **2002**, *124*, 14397-14402.
[46] Orgueira, H. A.; Fokas, D.; Isome, Y.; Chan, P. C. M.; Baldino, C. M. Regioselective synthesis of [1, 2, 3]-triazoles catalyzed by Cu (I) generated in situ from Cu (0) nanosize activated powder and amine hydrochloride salts. *Tetrahedron Lett*. **2005**, *46*, 2911-2914.
[47] Gardiner, M.; Grigg, R.; Kordes, M.; Sridharan, V.; Vicker, N. One-pot sequential and cascade formation of triazoles via palladium catalysed azide capture-1, 3-dipolar cycloaddition. *Tetrahedron*. **2001**, *57*, 7729-7735.
[48] Kamijo, S.; Jin, T.; Huo, Z.; Yamamoto, Y. Synthesis of triazoles from nonactivated terminal alkynes via the three-component coupling reaction using a Pd (0)− Cu (I) bimetallic catalyst. *J. Am. Chem. Soc*. **2003**, *125*, 7786-7787.
[49] Appukkuttan, P.; Dehaen, W.; Fokin, V. V.; Van der Eycken, E. A microwave-assisted click chemistry synthesis of 1, 4-disubstituted 1, 2, 3-triazoles via a copper (I)-catalyzed three-component reaction. *Org. Lett*. **2004**, *6*, 4223-4225.
[50] Feldman, A. K.; Colasson, B.; Fokin, V. V. One-pot synthesis of 1, 4-disubstituted 1, 2, 3-triazoles from in situ generated azides. *Org. Lett*. **2004**, *6*, 3897-3899.
[51] Kuruvalli, G.; Lavanya, L.; Pulakuntla, S.; Prashantha, C. N.; Shaik, A. H.; Reddyvari, H.; Vadamalai, V.; Reddy, V. D. Vitex negundo L. leaf extract suppresses the cell cycle and promotes apoptosis in colon cancer cells. *Indian. J. Biochem. Biophys.* **2024**, *61*, 269-278.
[52] Menteşe, E.; Yılmaz, F.; Baltaş, N.; Bekircan, O.; Kahveci, B. Synthesis and antioxidant activities of some new triheterocyclic compounds containing benzimidazole, thiophene, and 1, 2, 4-triazole rings. *J. Enzyme. Inhib. Med. Chem*. **2015**, *30*, 435-441.
[53] Chang, S. N.; Khan, I.; Kim, C. G.; Park, S. M.; Choi, D. K.; Lee, H.; Hwang, B. S.; Kang, S. C.; Park, J. G. Decursinol Angelate Arrest Melanoma Cell Proliferation by Initiating Cell Death and Tumor Shrinkage via Induction of Apoptosis. *Int. J. Mol Sci*. **2022**, *23*, 1629.
[54] Alshwyeh, H. A.; Al-Sheikh, W. M. S.; Rasedee, A.; Alnasser, S. M.; Al-Qubaisi, M. S.; Ibrahim, W. N. Mangifera indica L. kernel ethanol extract inhibits cell viability and proliferation with induction of cell cycle arrest and apoptosis in lung cancer cells. *Mol. Cell. Oncol*. **2024**, *11*, 2299046.
[55] Gouthami, K.; Veeraraghavan, V.; Nagaraja, P. In-silico characterization of phytochemicals identified from Vitex negundo (L) extract as potential therapy for Wnt-signaling proteins. *Egypt. J. Med. Hum. Genet*. **2022**, *23*, 1-15.
[56] Kumari, D.; Vhanmane, V. R.; Gouthami, K.; Reddy, V. D.; Nagendra, G. 2-DPC Mediated Effective Synthesis of Peptide Conjugates, their Antifungal and Antibacterial Properties. *ChemistrySelect* **2024**, *9*, e202402123.

[57] Bandlapalli, S.; Kalla, R. M. N.; Palakollu, V. N.; Kuruvalli, G.; Reddy, V. D.; Dahlous, K. A.; Lee, J. Synthesis, anti-microbial, and docking studies of functionalized chromenyl phosphonates using ionic liquid catalyst. *Mol. Divers.* **2024**, *1*, 13.

[58] Gouthami, K.; Veeraraghavan, V.; Lavanya, L.; Prashantha, C. N. Molecular docking studies for Vitex negundo (L) leaf extract compounds against Wnt-signalling proteins towards the treatment of colon cancer. *Chem. Data. Coll.* **2022**, *38*, 100829.

[59] Khan, M. A. A. M.; Ahsan, A.; Khan, M. A.; Sanjana, J. M.; Biswas, S.; Saleh, M. A.; Gupta, D. R.; Hoqu, M. N.; Sakif, T. I.; Rahman, M. M.; Islam, T. In-silico prediction of highly promising natural fungicides against the destructive blast fungus Magnaporthe oryzae. *Heliyon* **2023**, *9*, e15113.

[60] Rubin, E.; Shan, K. S.; Dalal, S.; Vu, D. U. D.; Milillo-Naraine, A. M.; Guaqueta, D.; Ergle, A. Molecular targeting of the human epidermal growth factor receptor-2 (HER2) genes across various cancers. *Int. J. Mol. Sci.* **2024**, *25*, 1064.

[61] Lee, K. J.; Oh, Y. C.; Cho, W. K.; Ma, J. Y. Antioxidant and anti-inflammatory activity determination of one hundred kinds of pure chemical compounds using offline and online screening hplc assay. *Evid. Based. Complement Alternat. Med.* **2015**, 165457.

[62] Augsten, L. V.; Göethel, G.; Gauer, B.; et al. Antiproliferative activity and toxicity evaluation of 1,2,3-triazole and 4-methyl coumarin hybrids in the MCF7 breast cancer cell line. *RSC Med. Chem.* **2023**, *14*, 869-879.

[63] Prashantha, C. N.; Gouthami, K.; Lavanya, L.; Bhavanam, S.; Jakhar, A.; Shakthiraju, R. G.; Suraj, V.; Sahana, K. V.; Sujana, H. S.; Guruprasad, N. M.; Ramachandra, R. Molecular screening of antimalarial, antiviral, anti-inflammatory and HIV protease inhibitors against spike glycoprotein of coronavirus. *J. Mol. Graph.* **2021**, *102*, 107769.

[64] Kanu, V. R.; Pulakuntla, S.; Kuruvalli, G.; Aramgam, S. L.; Marthadu, S. B.; Pannuru, P.; Hebbani, A. V.; Desai, P. P. D.; Badri, K. R.; Vaddi, D. R. Anti-atherogenic role of green tea (*Camellia sinensis)* in South Indian smokers. *J. Ethnopharmacol.* **2024**, *332*, 118298.

[65] Held, M.; Metzner, P.; Prinz, J. H.; Noé, F. Mechanisms of protein-ligand association and its modulation by protein mutations. *Biophys. J.* **2011**, *100*, 701-710.